RETROFITTING A LARGE STEAM TURBINE WITH A MECHANICALLY CENTERED SQUEEZE FILM DAMPER

by

Stephen L. Edney

Group Leader, Stress and Vibration

Dresser-Rand Energy Systems

Wellsville, New York

and

John C. Nicholas

President and Chief Engineer

Rotating Machinery Technology, Inc.

Wellsville, New York

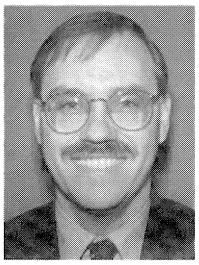

Stephen L. (Steve) Edney is Group Leader of the Stress and Vibration group at Dresser-Rand Energy Systems, in Wellsville, New York. In this capacity, he is responsible for providing technical support in rotordynamics and stress analysis. This includes directing evaluation on rerate inquiries of existing machines, troubleshooting field and shop problems, and conducting research programs.

Dr. Edney has 16 years of industrial experience, including the past eight years with Dresser-Rand. He started his career at GEC-Alsthom in the United Kingdom. He holds one U.S. Patent and has authored technical papers covering the finite element modeling of shafts, the nonlinear response of rotor bearing systems to shock excitation, and turbulence in tilting pad journal bearings.

Dr. Edney received his B.Sc. (1983) and Ph.D. (1990) degrees in Mechanical Engineering from the University of Nottingham, England. He is a member of ASME and the Vibration Institute, and a graduate member of the IMechE.

John C. Nicholas is part owner, President, and Chief Engineer of Rotating Machinery Technology, Inc., a company that repairs and services turbomachinery, and manufactures bearings and seals. He has worked in the turbomachinery industry for 22 years in the rotor and bearing dynamics areas, including five years at Ingersoll-Rand and five years as the Rotordynamics Group Supervisor at the Steam Turbine Division of Dresser-Rand.

Dr. Nicholas holds patents for a stabilized double pocket sleeve bearing design and a spray bar blocker design that lowers tilting pad bearing operating temperatures. He has authored over 30 technical papers concerning tilting pad bearing design, pressure dam bearings, rotordynamics, and support stiffness effects on critical speeds.

Dr. Nicholas received his B.S.M.E. degree from the University of Pittsburgh (1968) and his Ph.D. degree from the University of Virginia (1977) in rotor and bearing dynamics. He is a member of ASME, STLE, and the Vibration Institute.

ABSTRACT

Reviewed is the application of a squeeze film damper to a large steam turbine that addresses high vibration passing through the first critical speed. The turbine was the fifth near identical machine purchased over the course of several expansion projects at a large LNG plant. The original machine was designed in the early 1970s, and had a highly responsive first critical speed with an amplification factor in the upper teens. With a rotor this sensitive to unbalance, heavy rubs and operational difficulties were often encountered during start up and shut down transients. For the fifth machine, it was inquired how the rotor's response sensitivity could be improved without compromising rotor interchangeability with the sister units. A squeeze film damper bearing, being the only practical solution, was proposed and implemented.

The design and analysis methodology used in the development of the squeeze film damper bearing is discussed. To maintain rotor interchangeability, the design covers how the damper bearing was optimized to fit the available limited envelope. The systematic analytical approach demonstrates the importance of including support stiffness effects beyond the damper bearing. Test results are presented that illustrate the accuracy of the analysis, and the reduction in synchronous rotor response at the first critical speed.

INTRODUCTION

Squeeze film dampers in industrial turbomachinery are more typically used in higher speed machines to control the synchronous response and subsynchronous instability problems not adequately handled by conventional bearings. One recent application is reported in Leader, et al. (1995), where an 1109 lb steam turbine rotor operating on tilting pad bearings was retrofitted with squeeze film dampers that were centered by O-rings. This application was successful in reducing synchronous vibration amplitudes at the rotor's first critical speed by over 70 percent.

Many squeeze film damper publications exist in the literature, including Gunter, et al. (1975), in which the fundamental damper theory is outlined. Current research includes San Andres (1992), who concluded that a circumferentially "...grooved damper behaves at low frequencies as a single land damper of effective length equal to the sum of the land lengths and groove width." Development test results are presented in Kuzdzal, et al. (1996), that compare the effectiveness of several damper centering devices. The test vehicle used was a specially modified 10 stage high pressure barrel compressor with 4.0 inch diameter tilting pad journal bearings and dummy impeller wheels. The centering devices compared included various O-ring materials, a hanging

spring arrangement, and an arc spring. The authors concluded that "...an O-ring centered damper and a mechanical spring centered damper, both with eccentricities of zero, performed well to suppress subsynchronous vibration." A squeeze film damper tutorial containing a historical perspective, design and analysis procedures, and application examples is given in Zeidan, et al. (1996).

Discussed herein is the retrofit of a large steam turbine with a squeeze film damper to address transient vibration concerns on passing through the rotor's critical speed range. This machine was the fifth near identical unit purchased over the course of several expansion projects at a large LNG plant. The first machine was designed in the early 1970s and, although it conformed to then current rotordynamics guidelines, had a highly responsive first critical speed with an amplification factor in the upper teens. With a rotor this sensitive to unbalance, heavy rubs and operational difficulties were often encountered during start up and shut down transients, which was a major concern to the end user. For the fifth machine, it was inquired how the rotor's response sensitivity could be improved without compromising rotor interchangeability with the sister units. A squeeze film damper bearing, being the only practical solution, was proposed and implemented.

The design and analysis methodologies used in the development of the squeeze film damper bearings are described. Analytical and test results are presented that demonstrate the predicted and measured improvement in the rotor's transient response characteristics with the squeeze film damper as compared with a conventional bearing design. Since the rotor weighed 15,214 lb, a damper centered by O-rings was impractical. Thus, an arc spring design similar to that described in Kuzdzal, et al. (1996), was used as the centering device.

STEAM TURBINE APPLICATION

A cross sectional view of the steam turbine is shown in Figure 1, while Figure 2 is a photograph of the turbine on the test stand. The turbine is a condensing design with a controlled extraction delivering 12.5 MW at 3000 rpm, flexibly coupled to a two pole generator. The rotor comprises a forged shaft with 10 integral high pressure wheels and seven shrunk on low pressure wheels (Figure 3). The bearing span and mid-shaft diameter are 157.5 inch and 15.0 inch, respectively, yielding a L_b/D_s ratio of 10.5. In general, the flexibility of a rotor increases with the L_b/D_s ratio, yielding higher amplification factors and increased sensitivity to unbalance. The flexural stiffness of the rotor as approximated by beam theory is 948,000 lb/in.

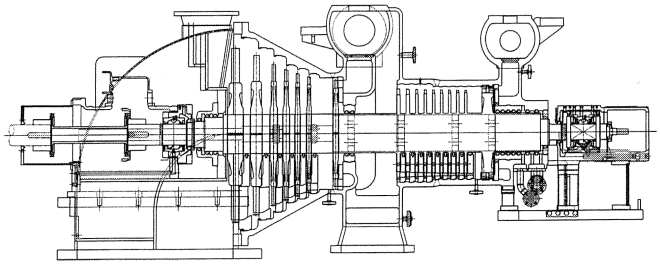

Figure 1. Cross Sectional View of Steam Turbine.

Evolution of Bearing Design

The first two machines, built in the early 1970s, were originally designed with spherically seated pressure dam sleeve bearings and a continuously lubricated gear type coupling. The steam end bearing was 6.0 inch in diameter by 5.73 inch long with a static bearing load of 177.0 psi, and the exhaust end bearing 8.0 inch in diameter by 6.0 inch long with a static bearing load of 193.3 psi. As a general rule of thumb, the combined bearing stiffness of a well designed rotor bearing system generally should be less than twice that of the shaft. The individual stiffnesses of these bearings were

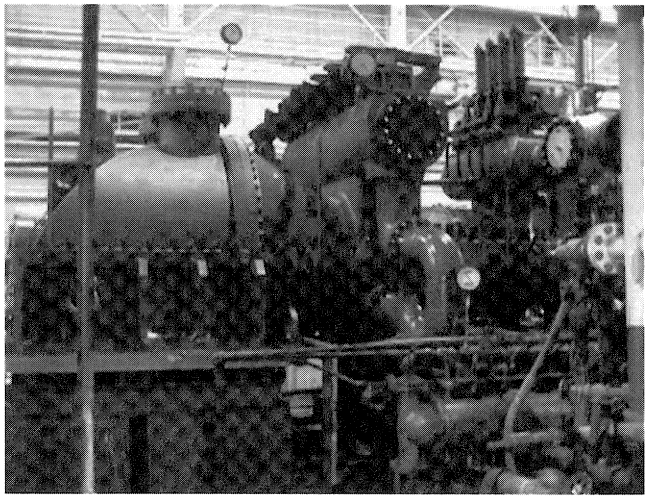

Figure 2. Steam Turbine on Test Stand.

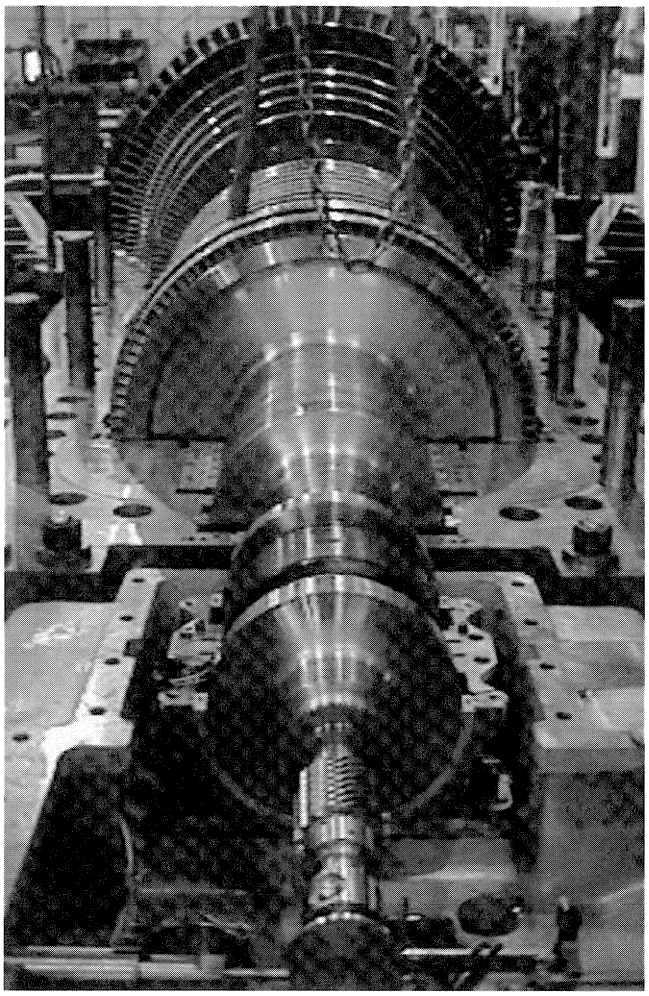

Figure 3. Steam Turbine Rotor in Lower Half Case.

in the 5,000,000 lb/in range that, clearly, did not meet this criterion. The steam end journal was straddled by a double collar nonequalizing tilting pad thrust bearing with a total area of 48 in^2 per side.

The sleeve journal bearings were retrofitted with titling pad designs in the mid 1980s. The design selected was a five pad load between pivot configuration. The pad axial lengths were reduced to 4.5 inch at the steam end and 5.5 inch at the exhaust end, yielding

increased static bearing loads of 231 psi and 204 psi, respectively. Although this retrofit resulted in some improvement in the rotor's transient response characteristics, operational difficulty was still experienced on passing through the first critical speed. This was because the individual bearing stiffnesses were almost the same as the original bearing designs. Ideally, an increase in the tilting pad axial length should have been used to decrease the static bearing loads, thereby yielding a softer hydrodynamic oil film. This, in turn, would have decreased the bearing's stiffness characteristics and provided increased effective damping as reported in Nicholas, et al. (1982). However, dimensional constraints of the original housings limited the axial length of the tilting pad retrofits that could be accommodated. This same bearing configuration was also used on the third and fourth machines supplied in the early 1990s. On these two machines, the coupling was upgraded to a dry diaphragm type.

The contract for the fifth machine was awarded in August 1997. At this time, an inquiry was made regarding how the rotor's response sensitivity at the first critical speed could be improved. To maintain interchangeability with the sister units, a modification to the rotor was not an option. Similarly, there was very little that could be done to further optimize the dynamic characteristics of the journal bearings. Consequently, squeeze film damper bearings, being the only practical solution, were proposed and implemented.

Squeeze Film Damper Design

A schematic and a photograph of the steam end squeeze film damper bearing are shown in Figures 4 and 5, respectively. The inner bearing is a tilting pad design comprising four pads oriented in the load between pivot configuration. Although the stiffness and damping characteristics of this bearing by itself are not too different compared with a five pad design, this configuration was chosen due to symmetry considerations that help to reduce overall response levels as documented in Nicholas, et al. (1982). The inner bearing is supported and centered in the housing by an arc spring, which is bolted into the housing at the horizontal split. Ground shims placed at the housing shoulder underneath the arc spring seat at the bolted joint were used to facilitate centering. A small controlled radial clearance was left between the housing and inner bearing to provide the cavity for the squeeze film damping action. Oil was supplied to this cavity and the inner bearing via an annular groove machined into the housing. The inner bearing is free to float in this cavity filled with oil and enclosed by O-ring end seals. The outside diameter of the inner bearing forms the damper journal, which is prevented from spinning by an antirotation pin. This is required to allow the inner bearing or damper journal to whirl but not spin in a precession motion, thus squeezing the oil in the small annular clearance that in turn generates an oil film pressure and, subsequently, a damping force. At the steam end, space constraints of the original housing and the fixed thrust collar locations limited the optimization of the damper design. This was less of an issue at the exhaust end, although the centerline of the bearing was moved outboard by 0.625 inch.

As a precaution, back up rigidly mounted conventional bearings (hereafter referred to as the rigid bearing design) were built in the event that the squeeze film damper did not perform as expected. These bearings had an identical tilting pad geometry to those used in the damper design, except that the outside diameter of the shell was oversized so that they could be simply rolled into the housing after removal of the arc spring to provide a rigid fit. The thrust bearing was also upgraded to a self-equalizing, directed lubrication design with increased area.

SQUEEZE FILM DAMPER THEORY

The principal concept of a squeeze film damper is to dissipate a rotor's vibration energy by optimizing the available damping. Since damping, however, is also a dynamic stiffness, just adding damping to a rotor supported on stiff bearings in most cases simply

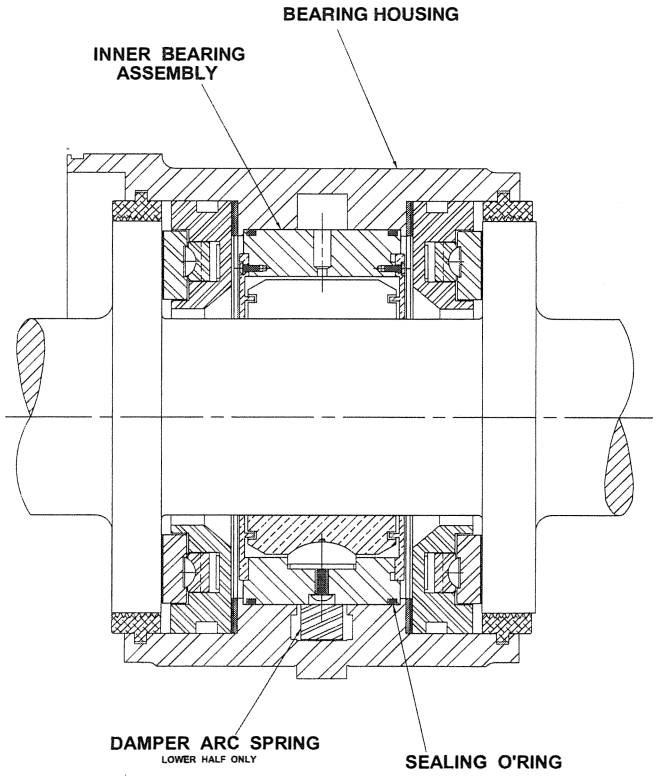

Figure 4. Steam End Squeeze Film Damper Bearing Schematic.

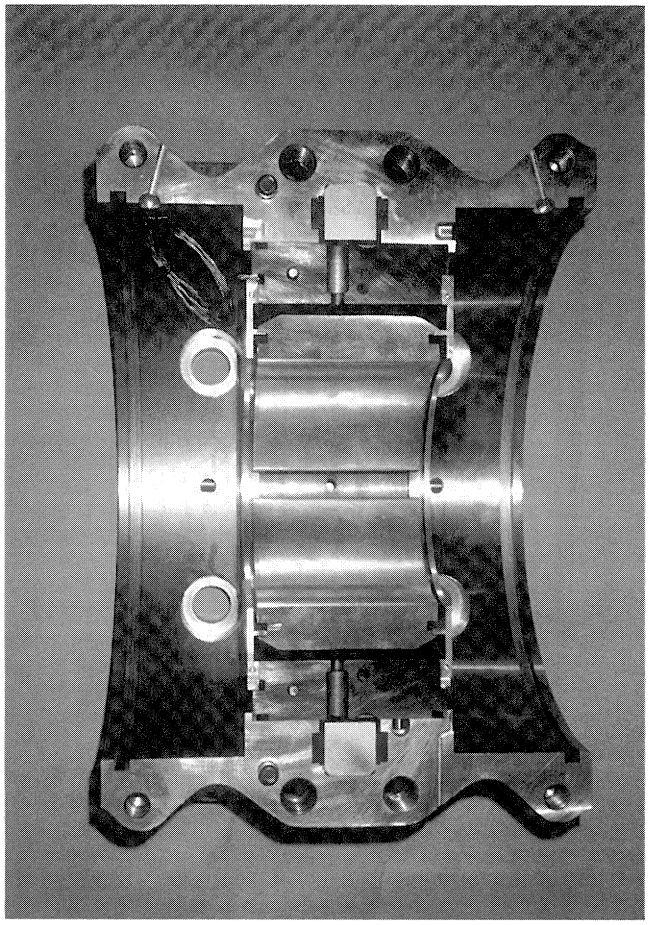

Figure 5. Steam End Squeeze Film Damper Bearing Photograph.

will not work. One of the key features in the successful design of a squeeze film damper is the introduction of flexibility in the bearing support structure. Allowing the bearing to move increases the available oil film damping, and, hence, its ability to remove vibration energy in the form of heat and thus reduce rotor response amplitudes. Other benefits include lower bearing transmitted forces and longer bearing life, particularly in the case of machinery operating above the first critical speed. Squeeze film dampers are typically used to reduce synchronous response levels at critical speeds and to solve unstable subsynchronous vibration problems.

A squeeze film damper is essentially a plain journal bearing in which only radial motion is allowed. Referring to Figures 4 and 5, this is achieved by providing an annular clearance between the outside diameter of the inner bearing and the inside diameter of its housing. The inner bearing is allowed to float in this cavity filled with oil and enclosed by O-ring end seals. The outside diameter of the inner bearing forms the damper journal, which is prevented from spinning by a loose antirotation pin. This is required to allow the inner bearing or damper journal to whirl but not spin in a precession motion, thus squeezing the oil in the small annular clearance that in turn generates an oil film pressure and, hence, a damping force. For optimum damping, a centering device of the inner bearing is often incorporated into the design. O-rings are the simplest devices typically used on machines with lightweight rotors, as in Leader, et al. (1995). Machines with heavy rotors, however, present a unique challenge requiring a mechanical element that can support a large weight and yet retain some inherent flexibility.

The theory on which many squeeze film damper analyses are based was originally developed by Gunter, et al. (1975). A circumferential groove is commonly machined into the housing to facilitate the supply of oil to the inner journal bearing. On mechanically centered damper bearings, this groove can also be used to retain the centering device as utilized in this application. With this design, the pressure profile generated by a radial squeezing motion, shown in Figure 6, is equivalent to that for a plain land without an oil groove and without end seals. Consequently, the values for total force, stiffness, and damping are also the same. It was also assumed that the damper would be precessing in steady-state circular motion, and, due to the low oil supply pressure, that the oil film would be cavitated. The equations used for stiffness and damping were those derived in Gunter, et al. (1975):

$$K_d = \frac{2\,\mu\,R\,L^3\,\varepsilon\,\omega}{c^3\,(1-\varepsilon^2)} \tag{1}$$

$$C_d = \frac{\pi\,\mu\,R\,L^3}{2\,c^3\,(1-\varepsilon^2)^{3/2}} \tag{2}$$

where:
ω = Shaft speed
R = Damper radius
L = Damper axial length
C = Damper radial clearance
ε = Damper eccentricity ratio
μ = Oil viscosity

In addition to the oil film stiffness and damping, the stiffness of the centering device also has to be included to accurately represent the squeeze film damper characteristics.

ARC SPRING DESIGN

The centering device shown in Figure 7 is essentially an arc spring similar to that presented in Kuzdzal, et al. (1996). It has a semicircular profile and is retained in the housing at the horizontal split by bolts at both ends. At bottom dead center, the inside radius of the arc spring has a raised saddle with line contact at the inner bearing to provide support in the vertical direction only. The arc spring is designed with a predetermined stiffness and is preloaded

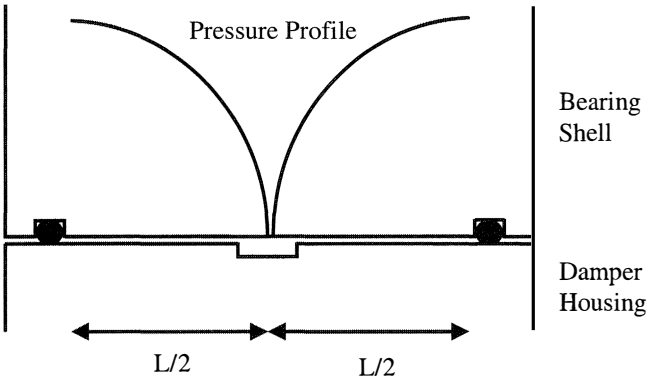

Figure 6. Axial Pressure Profile of a Squeeze Film Damper with End Seals.

to offset half the rotor weight to center the inner bearing in the housing. Ground shims placed at the horizontal joint between the housing and arc spring are used to facilitate this. The challenge in the case of a large heavy rotor, however, is to design an arc spring that is flexible enough to allow the damper to work and yet strong enough to prevent the damper from bottoming out, and not to yield or fatigue under load. For this reason, a high strength material, ASTM 4340, was used for the arc spring.

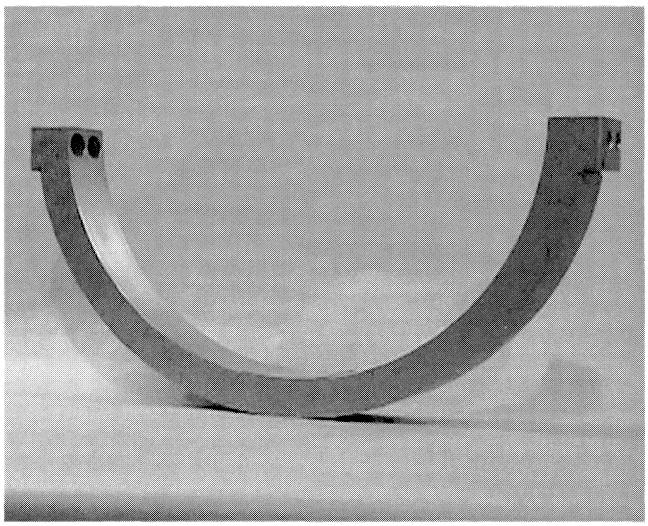

Figure 7. Exhaust End Damper Bearing Arc Spring.

Analysis Methodology

A good approximation of the stiffness of an arc spring can be obtained by applying Castigliano's second theorem for a symmetrical curved beam from Roark's Formulas, Young (1989). While this method can easily and adequately be used for preliminary estimates, a more accurate calculation is appropriate for the final analysis. The best approach is a finite element simulation in which the effects of bolted joints, etc., can be more accurately represented.

This approach was followed. A spreadsheet was written with the closed form equations for deflection, stiffness, and bending stress (APPENDIX A) programmed as a function of static load, inner arc radius, outer arc radius, and axial width. This allowed various arc spring geometries to be quickly evaluated and optimized for each application. The spreadsheet also contained a section that calculated the fatigue strength of the arc spring under alternating load conditions. The value used for alternating load was equal to one times the force of gravity (1G), unless this yielded a deflection that exceeded the radial clearance of the damper. In this case, the

load used was that which would produce a deflection equal to the damper radial clearance.

For example, the dimensions selected for the exhaust end arc spring were: 6.812 inch inner arc radius, 7.859 inch outer arc radius, and 1.75 inch axial width for a static load of 8976 lb. With these values, the calculated deflection and stiffness were 0.0083 inch and 1,084,000 lb/in, respectively, with a maximum tensile stress of 31,888 psi.

In reality, however, the actual static deflection and, hence, stiffness are dependent on how securely the arc spring can be attached in the housing. For example, the inherent flexibility at the bolted joints will result in both an increase in the static deflection and a reduction in the overall stiffness. For these reasons, a more accurate simulation of the final geometry selected is necessary. In this case, a finite element model was constructed. The mesh developed is shown in Figure 8 and comprises a three dimensional solid model of eight node brick elements. A half model only was constructed by virtue of symmetry. Translational displacement constraints were applied horizontally at the cut surface of the saddle, and vertically along the inner edge of the housing seat. The bolts were modeled using a beam element of equivalent stiffness. A downward vertical load one half the static weight supported by the spring was distributed along the line of contact at the saddle.

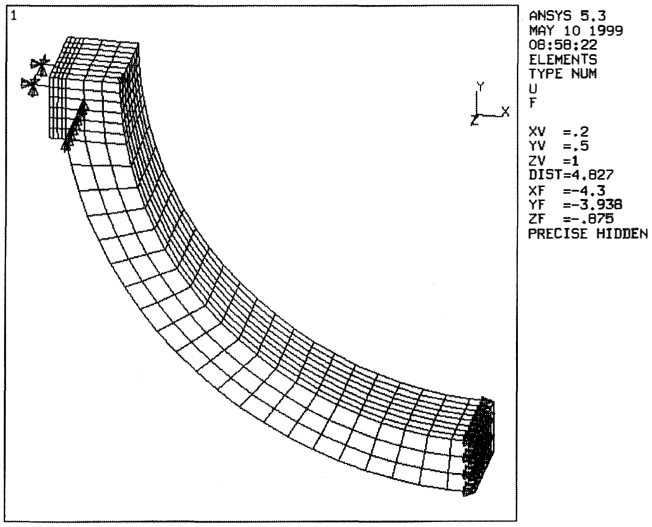

Figure 8. Finite Element Mesh of Half Arc Spring Model.

The resultant deflected shape is shown in Figure 9. The deflection at the saddle is 0.01095 inch compared with the 0.0083 inch calculated using Castigliano's theorem. This is equivalent to roughly a 30 percent increase in deflection, which is significant when one considers the centering accuracy required for the damper. Furthermore, the extent to which the arc spring deflects inward is quite apparent. This is an important consideration in the design of the arc spring, since if the deflection is sufficient to cause contact with the inner bearing shell, the stiffness and, hence, damper performance characteristics will be significantly altered.

This method also provides more appropriate stress data for a fatigue calculation. The value used for mean stress was the maximum equivalent or Von Mises stress when statically loaded. These results are shown in Figure 10, with the maximum value of 31,054 psi located at the outside fiber where the load is applied. The assumed alternating stress is a worst case value, given by the load that would displace the arc spring beyond the statically loaded condition an amount equal to the damper radial clearance; in this case, 17,016 psi. The values are plotted on the Goodman diagram shown in Figure 11. The arc spring material is ASTM 4340 of minimum ultimate tensile strength, 160,000 psi, and minimum yield strength, 140,000 psi. The endurance limit corrected for

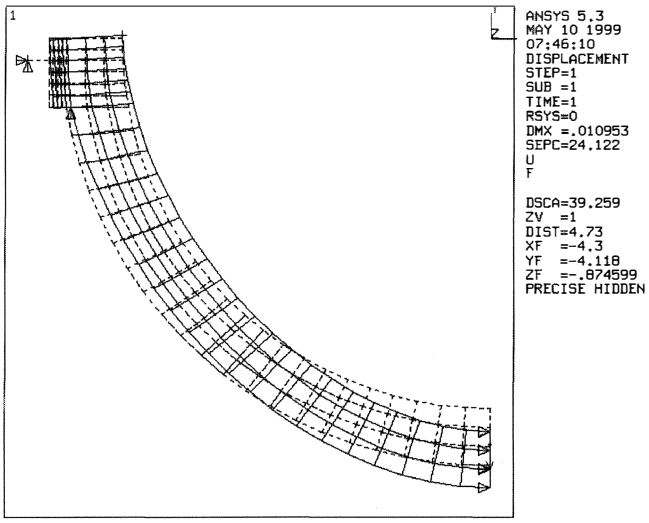

Figure 9. Boundary Conditions and Statically Deflected Shape.

surface, size, load, temperature, and miscellaneous effects is 39,900 psi. These values yield a safety factor of:

$$1/n = \sigma_a / \sigma_e + \sigma_m / \sigma_{ut} = 0.62 \quad \text{or} \quad n = 1.6 \tag{3}$$

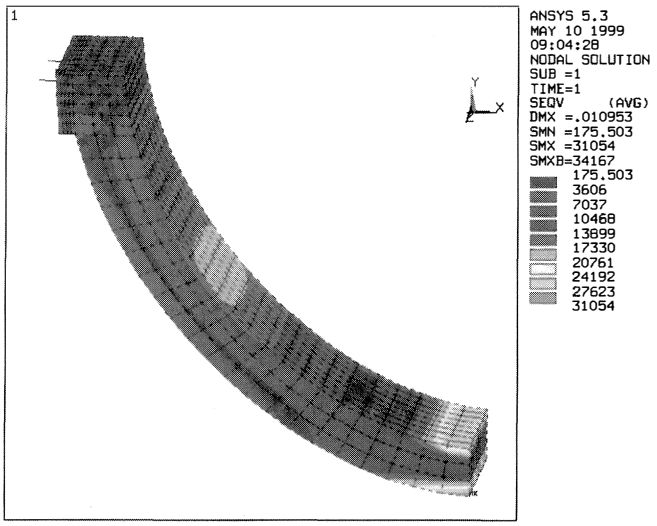

Figure 10. Von Mises Stress Distribution.

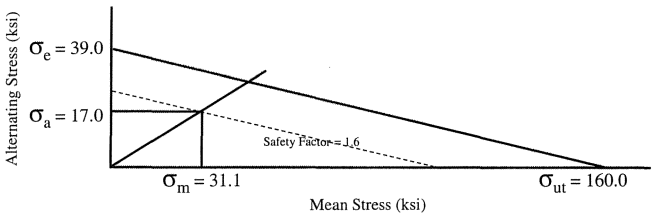

Figure 11. Goodman Diagram—Exhaust End Arc Spring.

Deflection Testing

The effectiveness of a damper is largely dependent on how well it is centered under load. The best means of achieving this is through static or deflection testing. The benefit is twofold, since both the deflection and stiffness can be accurately determined. In

this application, the test rig illustrated in Figure 12 was used. The bearing housing with arc spring installed was assembled around an arbor rigidly clamped between two solid end plates. The housing was inverted so that the saddle of the arc spring was in line contact with the arbor. Loads were applied to the housing using a hydraulic press, and measured using a calibrated load cell. The deflection of the housing was measured using two dial indicators, placed equal distance from either side of the line of contact between the arc spring and arbor. Two indicators were used to ensure that the housing did not roll as load was applied, thus producing erroneous results. The test was conducted twice to ensure repeatability and consistency in the data.

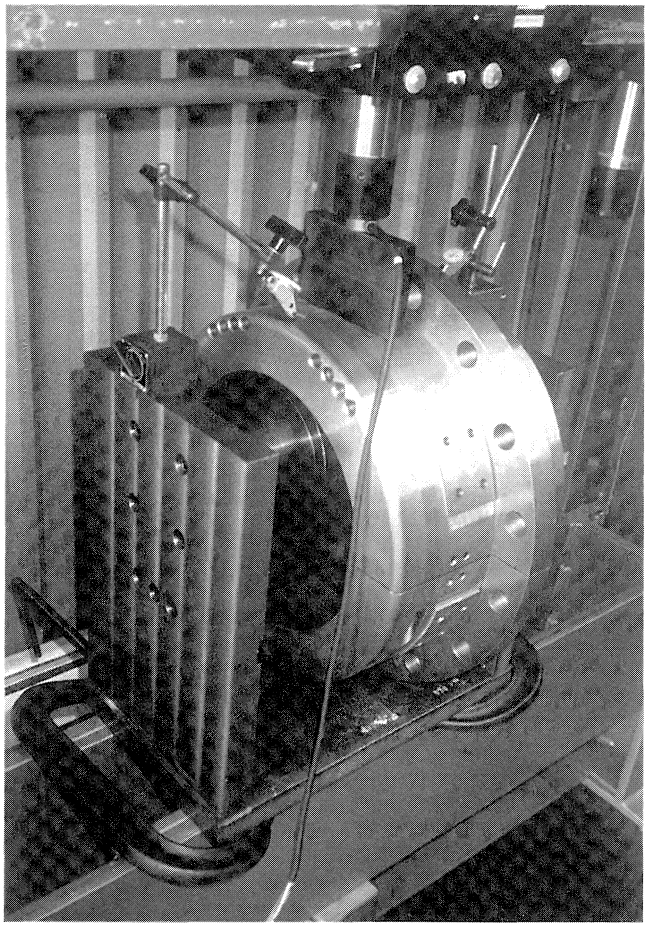

Figure 12. Arc Spring Deflection Test Rig.

The test results on the exhaust end arc spring are given in Figure 13. Both sets of data are in excellent agreement, with the difference in best fit stiffness of less than 0.4 percent. The deflection of 0.0107 inch at the design static loading compared well with the 0.01095 inch calculated from the finite element model. In the free condition, the vertical positions of the arc springs were offset with appropriate thickness shoulder shims. This offset was verified during the machine assembly, with plastigage impressions made of the damper radial clearance.

ROTORDYNAMICS ANALYSIS

From the actual steam turbine rotor shown in Figure 14, a mass elastic model was generated for the rotordynamics analysis. The model is illustrated in Figure 15, and the resulting undamped critical speed map in Figure 16. Included on the undamped critical speed map are dynamic stiffness curves at nominal bearing clearance for the squeeze film damper and rigid bearing designs. These curves are derived from a series combination of the squeeze

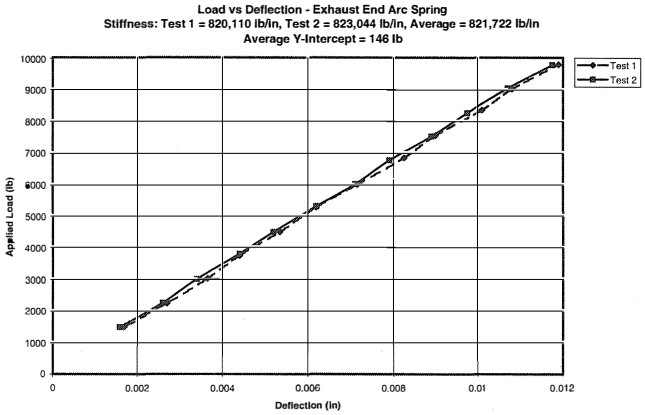

Figure 13. Load Versus Deflection Curve for Exhaust End Arc Spring.

film, bearing oil film, and support characteristics as shown in Figure 17 and outlined by Nicholas, et al. (1986). The largest effect is from the damper bearing, which has an effective stiffness of approximately one quarter of that of the rigid design. A conservative eccentricity ratio of 0.4 was used in the calculation of the damper stiffness and damping coefficients. Values of 5.0×10^6 lb/in and 500 lb were used for the support stiffness and mass at each bearing, with 10 percent critical damping as in Nicholas, et al. (1986). The steam end arc spring in the lower half bearing housing is shown in Figure 18, and supporting the tilting pad journal bearing in Figure 19.

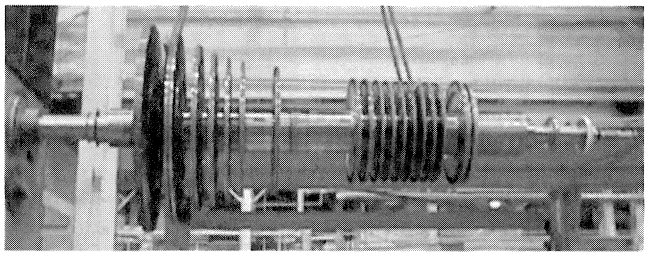

Figure 14. Steam Turbine Rotor.

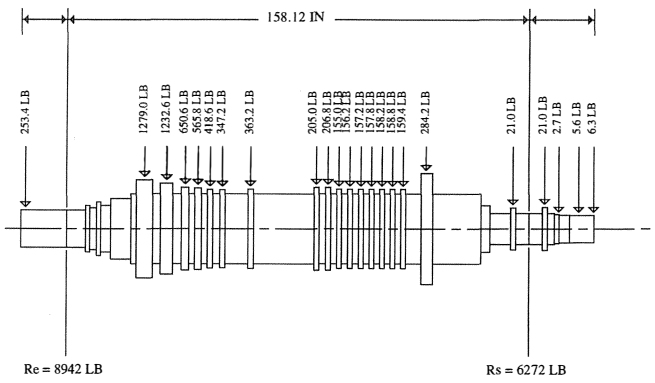

Figure 15. Mass Elastic Model of Rotor.

Unbalance Response

The predicted synchronous amplitude and phase lag versus speed plots, with and without the squeeze film damper, are compared in Figures 20 and 21 for a first mode excitation, and Figures 22 and 23 for a second mode excitation. The response plots are at the steam and exhaust end radial probes located on the right-hand side of the machine as viewed from the governor. The probes

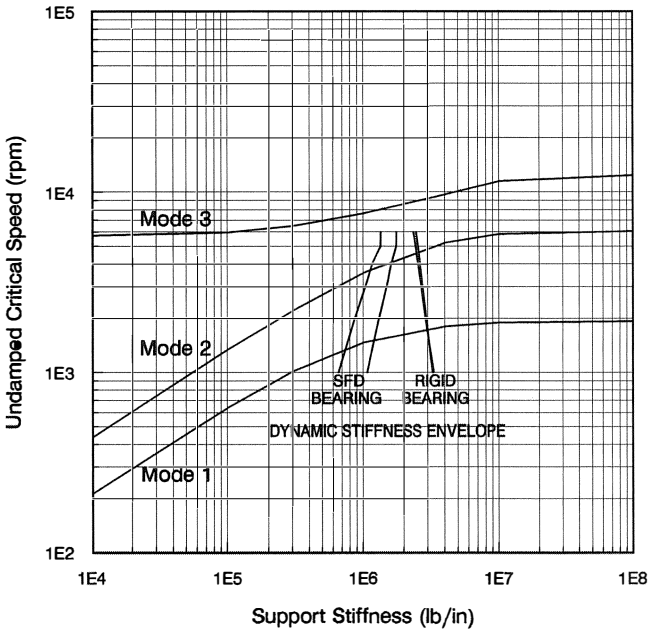

Figure 16. Undamped Critical Speed Map.

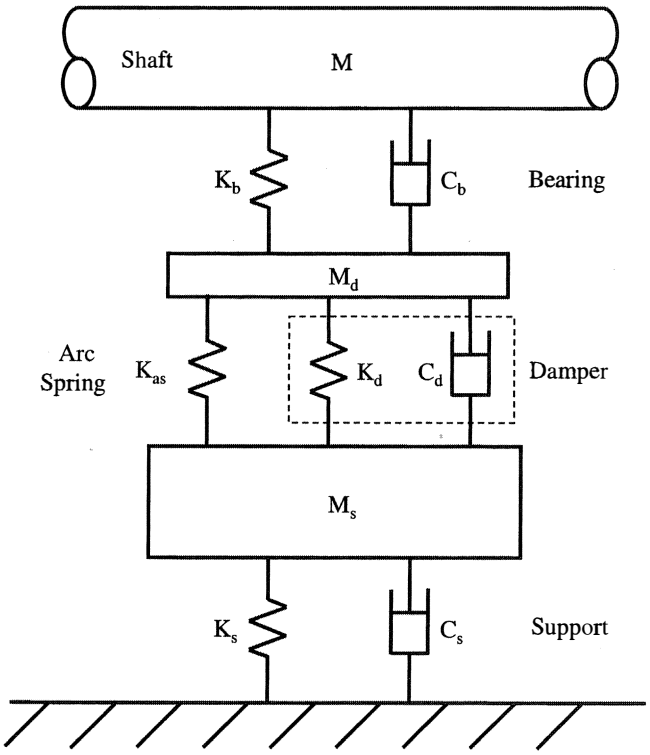

Figure 17. Idealization of Bearing-Damper-Support Characteristics.

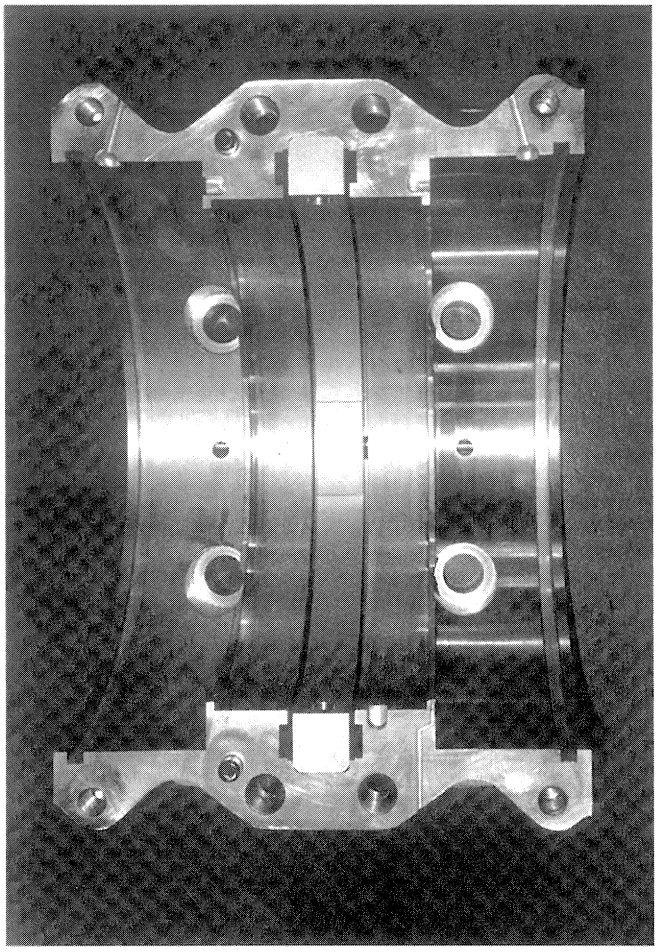

Figure 18. Steam End Arc Spring in the Lower Half Housing.

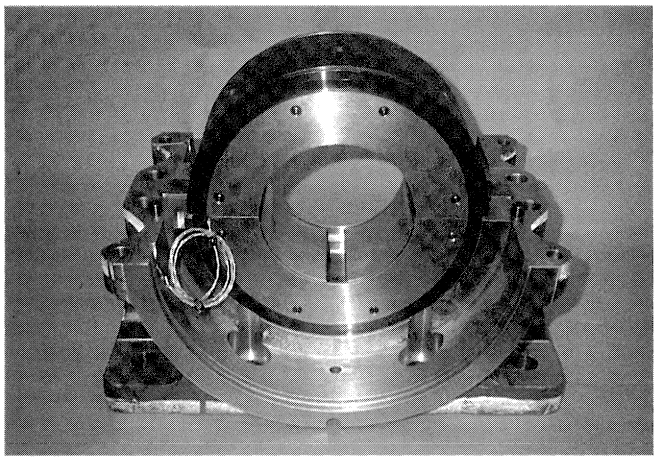

Figure 19. Steam End Tilting Pad Damper Bearing and Arc Spring in the Lower Half Housing.

are located inboard of the journal bearing at the steam end, and outboard at the exhaust end. The first mode was excited with an unbalance of 100 oz-in (or roughly 20W/N, where W is the rotor weight and N is the synchronous operating speed of 3000 rpm) placed at the rotor's midspan. The second mode was excited by placing one half this unbalance just inboard of each journal bearing 180 degrees out-of-phase.

Values for critical speed, amplification factor, and maximum vibration amplitude are compared in Table 1. With the squeeze film damper, the first mode amplification factors and maximum amplitudes are lower by factors of at least three. It is noteworthy that the amplitudes at the exhaust end are less than at the steam end, particularly with the rigid bearings. This is due to the location of the exhaust end probes being outboard of the journal bearing and, hence, closer to a node point in this first mode unbalanced condition. This is illustrated in Figure 24, which compares the deflected shapes of the rotor at the first critical speed. This figure also helps in explaining the difficulty of controlling the rotor's

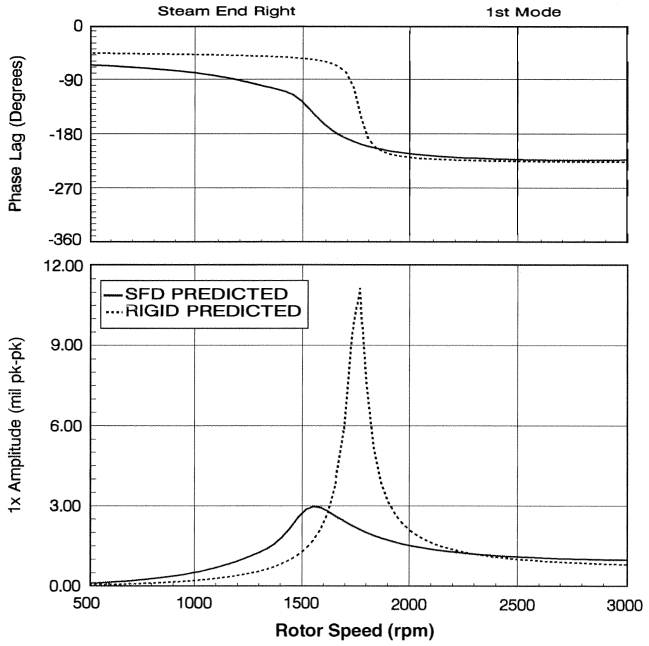

Figure 20. Predicted Amplitude and Phase Lag at Steam End Right Probe—First Mode Excitation.

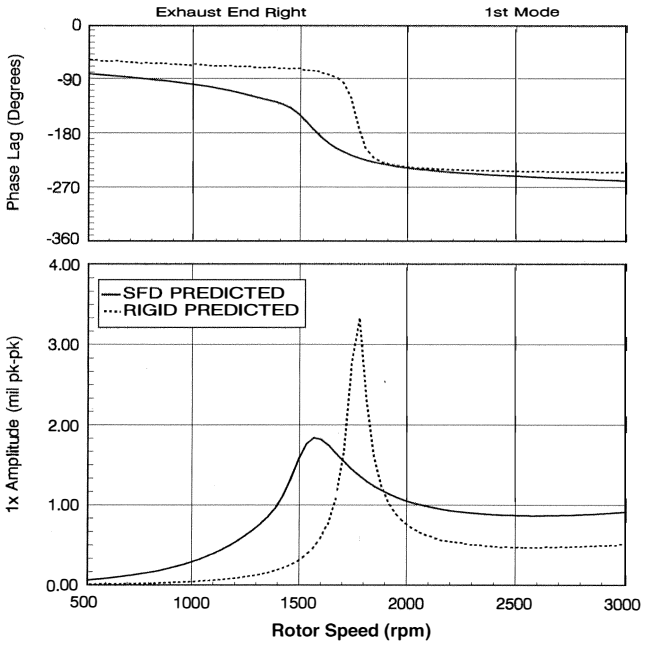

Figure 21. Predicted Amplitude and Phase Lag at Exhaust End Right Probe—First Mode Excitation.

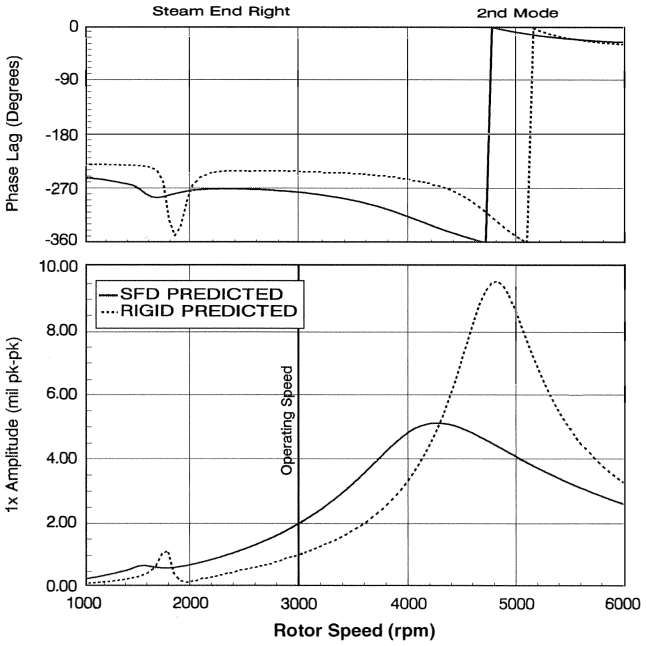

Figure 22. Predicted Amplitude and Phase Lag at Steam End Right Probe—Second Mode Excitation.

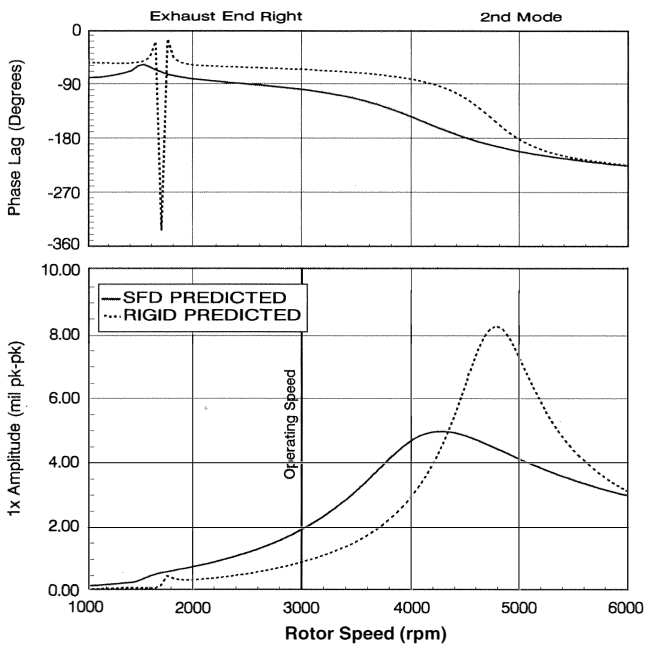

Figure 23. Predicted Amplitude and Phase Lag at Exhaust End Right Probe—Second Mode Excitation.

vibration with the rigid bearings. The locations of the nodal points are determined by the relative flexibility of the rotor compared with the resultant support flexibility; with two consequences as the nodal points move closer to the bearings. First, the effective bearing damping is greatly reduced due to the restricted motion in the bearings, and second, the response amplitudes at the rotor's midspan are considerably greater than those indicated at the probes. This latter situation can lead to a potentially damaging rub condition if the midspan vibration amplitudes build up sufficiently to exceed the running clearances of the interstage seals. With the squeeze film damper, however, the nodal points are now sufficiently away from the bearings with enough relative amplitude to make the bearing damping more effective. On the other hand, one consequence with the squeeze film damper is that the operating speed vibration amplitudes will be slightly higher than with the rigid bearings, as illustrated in Figures 20 to 23.

The squeeze film damper influence on the second mode is less, with the values for amplification factor and maximum amplitude reduced by factors in the neighborhood of two. Although the second mode is highly damped, the concern with the application of a squeeze film damper is that the additional flexibility of the damper may cause a decrease in the second peak response speed. This might result in a second critical speed that may be lowered too close to the operating speed range. In this case, the peak response

Table 1. Comparison of Predicted Peak Response Speed (NC), Amplification Factor (AF), and Maximum Amplitude (A_{MAX})—Squeeze Film Damper Versus Rigid Bearings.

Mode	Steam End Right NC (rpm) / AF (dim) / A_{MAX} (mil)		Exhaust End Right NC (rpm) / AF (dim) / A_{MAX} (mil)	
	Damper	Rigid	Damper	Rigid
First	1585 / 5.2 / 2.96	1760 / 17.5 / 11.2	1550 / 5.6 / 1.83	1760 / 17.5 / 3.33
Second	4240 / 2.6 / 5.12	4790 / 5.9 / 9.56	4295 / 2.2 / 4.97	4790 / 5.9 / 8.23

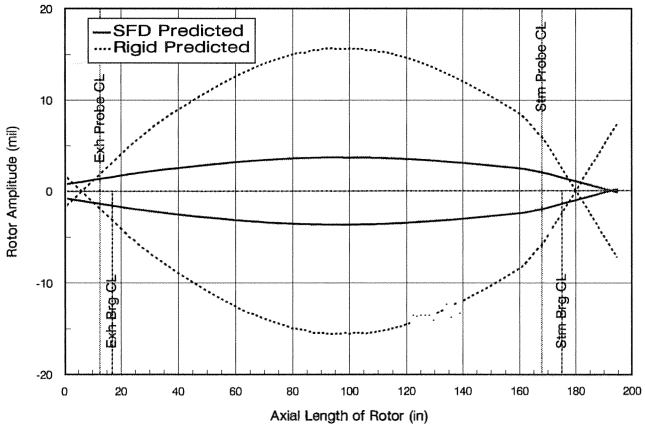

Figure 24. Predicted Deflected Shape at Critical Speed—First Mode Excitation.

was reduced by approximately 600 rpm, from 4800 to 4200 rpm, which, with an operating speed of 3000 rpm, is not a problem.

Stability

The results of an eigenvalue stability analysis with and without the squeeze film damper are compared in Table 2 at the synchronous operating speed of 3000 rpm. The values given for damped natural frequency and logarithmic decrement correspond to the first forward whirl mode. With the squeeze film damper, the dynamic stability is improved by a factor of greater than three.

Table 2. Comparison of Eigenvalue Analysis Results—Squeeze Film Damper Versus Rigid Bearings.

Bearing Design	Damped Natural Frequency (rpm)	Logarithmic Decrement (dim)
Damper	1503	0.42
Rigid	1730	0.13

EXPERIMENTAL VERIFICATION

For comparison, verification tests were conducted on both the squeeze film damper and rigid bearing designs. The primary shop test was conducted with the squeeze film damper bearings, and included an unbalance response test in addition to a four hour no load run test. Following the successful completion of this test, the damper bearings and arc springs were removed and replaced with the oversized or rigid bearings. A two hour run test only was conducted with these bearings.

Unbalance Response Verification Test

To validate the squeeze film damper bearing analysis methodology, an unbalance response test was conducted. Due to the lack of any accessible trim balance planes, this was achieved by placing a weight at the coupling hub. Although a coupling hub unbalance will not logically excite the first mode, the transient response characteristics will provide sufficient information to correlate the analytical model. On a flexible rotor such as this, test stand results from a coupling unbalance can be slightly misleading in that the rotor's inherent residual unbalance can be a dominating factor. More appropriate data, however, can be obtained by vectorially subtracting an as balanced set of data from the unbalance test results as described by Nicholas and Edney, et al. (1997). This method was used in the correlation of the analytical model.

For this test, the unbalance applied at the coupling hub was limited to four times the residual unbalance tolerance of 4W/N, where W is that portion of the rotor weight supported by the exhaust end bearing and N is the synchronous operating speed of 3000 rpm. The test results are compared with the analytical simulations in Figures 25 and 26. The vibration trends generally are in excellent correlation. The highest overall response amplitudes occur at the exhaust end probes, and are in almost exact agreement with the analysis. Table 3 compares the vectorially compensated response amplitudes at 3000 rpm. In general, both the response and phase trends are in good agreement, although the individual peaks and troughs appear to be underestimated by about 200 rpm. The implication is that the stiffness model of the rotor is too flexible. Most likely, the stiffening effect assumed at the shrunk on wheels is too low. At 3000 rpm, the difference between the predicted and measured amplitudes at the exhaust end probes is approximately 10 percent; although a difference of almost 50 percent is observed at the steam end probes.

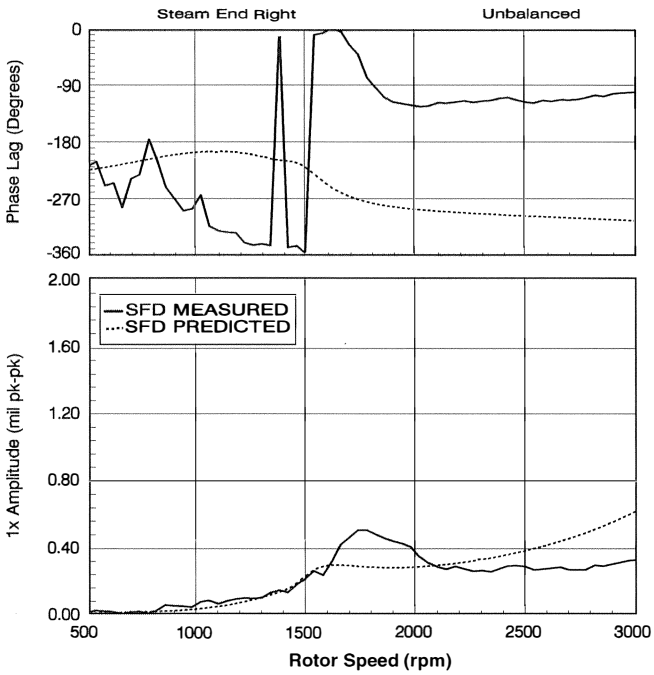

Figure 25. Predicted and Measured Amplitude and Phase Lag at Steam End Right Probe—Coupling Unbalance.

Squeeze Film Damper Versus Rigid Bearings

With the weight removed, the synchronous amplitude and phase lag versus speed plots of the as balanced rotor during a coast down are illustrated in Figures 27 and 28, with and without the squeeze film damper. Test results obtained from the probes located on the right-hand side of the machine are again compared. The response plots clearly show the location, amplification factor, and maximum amplitude of the peak response. These values are summarized in Table 4, along with the analytical predictions.

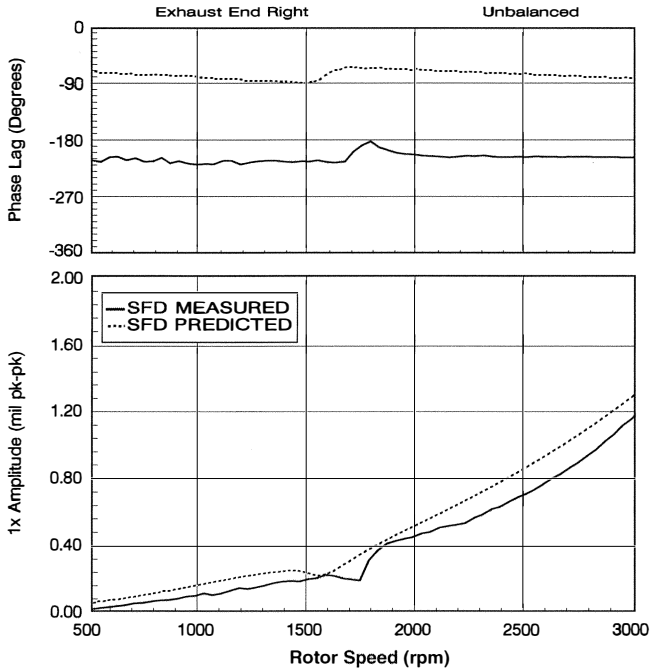

Figure 26. Predicted and Measured Amplitude and Phase Lag at Exhaust End Right Probe—Coupling Unbalance.

Table 3. Comparison of Predicted and Measured Amplitude at 3000 rpm (A_{MAX})—Damper Bearing with Coupling Unbalance.

	SE Left A_{MAX} (mil)	SE Right A_{MAX} (mil)	EE Left A_{MAX} (mil)	EE Right A_{MAX} (mil)
Measured	0.40	0.32	1.28	1.16
Predicted	0.78	0.60	1.44	1.29
% Error	48.7	46.7	11.1	10.1

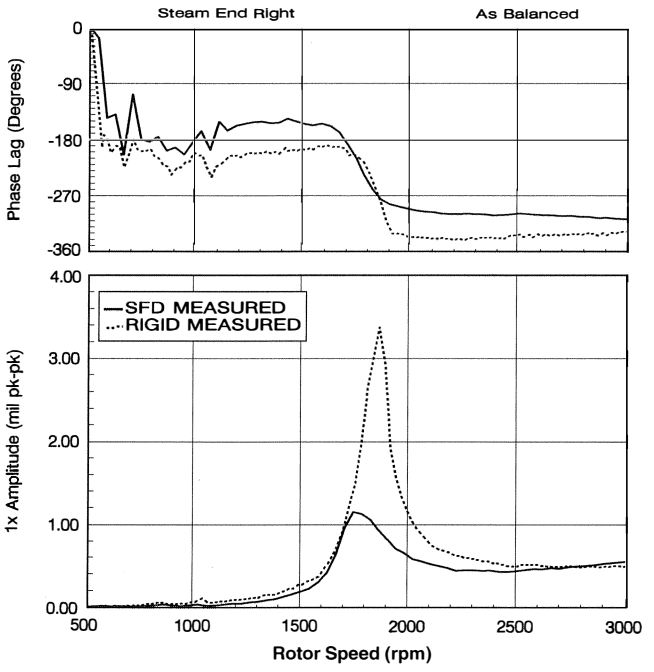

Figure 27. Comparison of Damper and Rigid Bearing Measured Amplitude and Phase Lag at Steam End Right Probe—As Balanced.

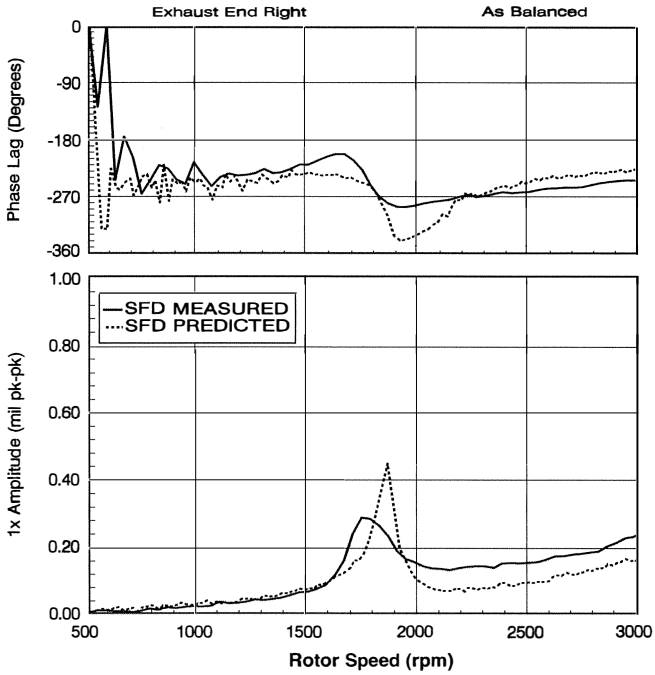

Figure 28. Comparison of Damper and Rigid Bearing Measured Amplitude and Phase Lag at Exhaust End Right Probe—As Balanced.

Table 4. Comparison of Measured and Predicted Peak Response Speed (NC), Amplification Factor (AF), and Maximum Amplitude (A_{MAX})—Squeeze Film Damper Versus Rigid Bearings.

	Steam End Right NC (rpm) / AF (dim) / A_{MAX} (mil)		Exhaust End Right NC (rpm) / AF (dim) / A_{MAX} (mil)	
	Damper	Rigid	Damper	Rigid
Measured	1740 / 7.6 / 1.15	1855 / 18.5 / 3.38	1740 / 7.9 / 0.28	1855 / 18.5 / 0.44
Predicted	1585 / 5.2 / 2.96	1750 / 17.5 / 11.2	1550 / 5.6 / 1.83	1760 / 17.5 / 3.33

The general trends of the response characteristics are excellent. The test results show a reduction in peak response amplitude with the squeeze film damper of 65 percent at the steam end (3.4 to 1.2 mils peak-to-peak from Figure 27) and 25 percent at the exhaust end (Figure 28). These values compare favorably with the analytical predictions of 70 percent and 45 percent at the steam and exhaust ends, respectively. The actual reduction in amplification factor associated with each peak response is roughly two, which is less than the three predicted. The location of the peak response is logically reduced with the squeeze film damper, although by only 100 rpm, not 200 rpm as predicted. Furthermore, the operating speed amplitudes with the squeeze film damper are slightly higher, as predicted. For ease of comparison, the squeeze film damper predicted response trends are shown normalized at the peak response to the measured results in Figures 29 and 30. Although the location of the measured peak response is higher than predicted by 200 rpm, the general shape of the response characteristics is in good correlation. Under predicting the critical speed with the damper design by 200 rpm may be caused by neglecting any hydrodynamic effect in the damper circumferential feed groove. From San Andres (1992), this groove may act as part of the damper land, thereby producing a higher stiffness than predicted and, thus, a slightly higher critical speed.

Nevertheless, all these trends indicate a significant improvement in the transient response characteristics of the rotor. Furthermore, the principal benefit will be a reduction in midspan vibration amplitudes at the peak response speed. Lower vibration amplitudes will reduce the possibility of minor transient rubs and unnecessary wear of interstage labyrinth seals, which was the primary objective in applying the squeeze film damper.

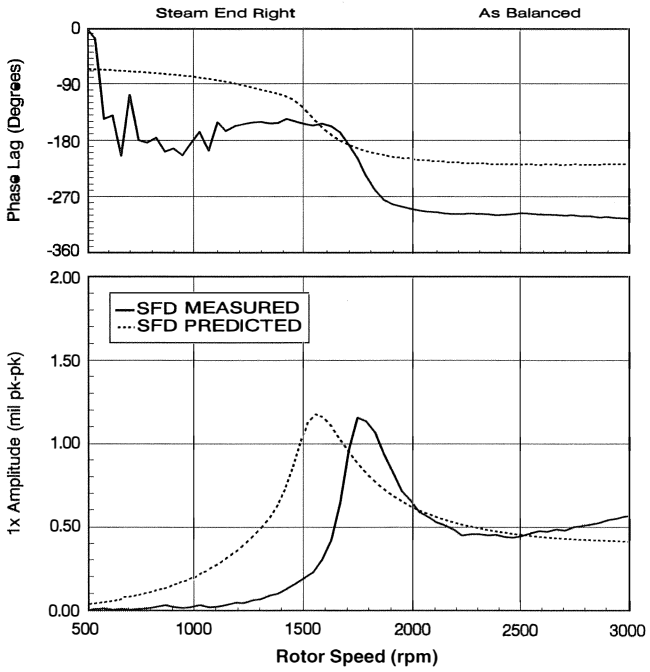

Figure 29. Normalized Squeeze Film Damper Measured Versus Predicted at Steam End Right Probe.

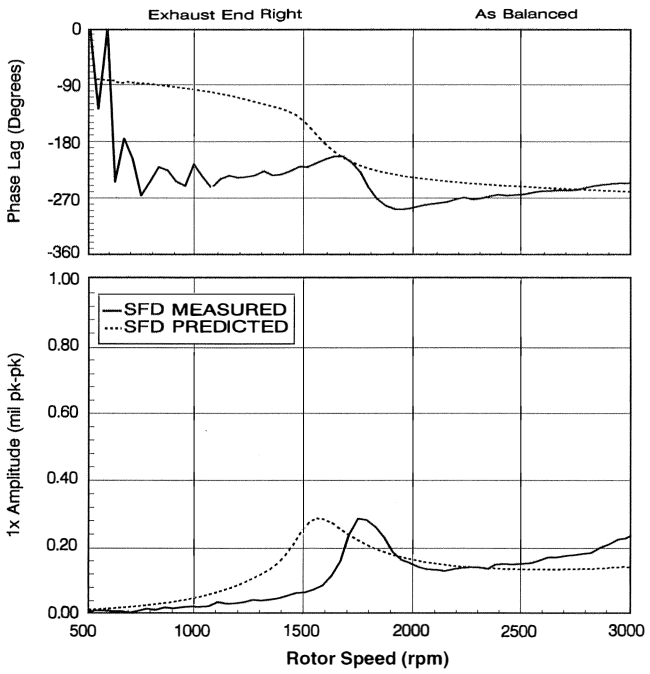

Figure 30. Normalized Squeeze Film Damper Measured Versus Predicted at Exhaust End Right Probe.

CONCLUSIONS

- The critical speed and stability characteristics of machines with sensitive or problem rotors can be greatly improved by modifying the bearings to incorporate a squeeze film damper. If performed carefully, this solution can be implemented relatively quickly and inexpensively compared with other options such as modifying the rotor and/or the case.

- Encasing a conventional bearing with a squeeze film damper lowers the resultant damping compared with that available in the conventional bearing. The overall stiffness, therefore, must also be lowered to allow rotor motion at the bearings in order to make the available damping more effective. The net benefits are lower amplification factors and reduced peak response amplitudes.

- The ability to accurately center squeeze film dampers in applications with relatively heavy rotors is a key factor in the successful performance of this design. With mechanical centering devices such as the arc spring used herein, the stiffness effects of bolted or hooked joints must be accounted for in determining the overall stiffness, and hence deflection, of the spring.

- Within the constraints of the existing bearing housing design in the application described, a significant improvement in the transient response characteristics of a large flexible steam turbine rotor was predicted and observed.

- A reduction in the measured peak response amplitudes with the squeeze film damper of 65 percent at the steam end (3.4 to 1.2 mils peak-to-peak) and 25 percent at the exhaust end were observed compared with the original rigid bearing design.

- The dynamic stability of a rotor supported on conventional bearings can be extended by the addition of a squeeze film damper.

NOMENCLATURE

A_{MAX} = Maximum amplitude (mil)
AF = Amplification factor at NC (dim)
c = Damper radial clearance (in)
C_b = Bearing damping (lb-sec/in)
C_d = Squeeze film damping (lb-sec/in)
C_s = Support damping (lb-sec/in)
D_x = Horizontal deflection (in)
D_y = Vertical deflection (in)
E = Elastic modulus (psi)
EE = Exhaust end
H = Horizontal load (lb)
I = Second moment of area (in^4)
K_{as} = Arc spring stiffness (lb/in)
K_b = Bearing stiffness (lb/in)
K_d = Squeeze film stiffness (lb/in)
K_s = Support stiffness (lb/in)
L = Damper axial length (in)
M = Journal mass (lb)
M_d = Damper mass (lb)
M_o = Bending moment (lb-in)
M_s = Support mass (lb)
n = Factor of safety (dim)
NC = Critical speed (rpm)
R = Damper radius (in)
R_a = Average arc spring radius (in)
SE = Steam end
V = Vertical load (lb)
ε = Damper eccentricity ratio (dim)
μ = Oil viscosity (lb-sec/in^2)
θ = Angular deflection (rad)
σ_a = Alternating stress (psi)
σ_e = Endurance limit (psi)
σ_m = Mean stress (psi)
σ_{ut} = Ultimate tensile strength (psi)
ω = Shaft speed (rad/sec)

APPENDIX A

Referring to Figure A-1, the following equations for displacement and angular rotation can be derived using Castigliano's second theorem, Young (1989):

$$D_y = \{(\pi/4)\, V\, R_a^3 + (1/2) H\, R_a^3 + M_o\, R_a^2\}/E\, I$$

$$D_x = \{(1/2)\, V\, R_a^3 + (3\pi/4-2) H\, R_a^3 + (\pi/2-1) M_o\, R_a^2\}/E\, I \quad \text{(A-1)}$$

$$\theta = \{V\, R_a^2 + (\pi/2-1) H\, R_a^2 + (\pi/2) M_o\, R_a\}/E\, I$$

Applying boundary conditions of $D_x = 0$ and $\theta = 0$ gives:

$$D_y = \{0.0234\ V\ R_a^3\} / E\ I \qquad \text{(A-2)}$$

The vertical stiffness can then be derived from:

$$K_s = V / D_y \qquad \text{(A-3)}$$

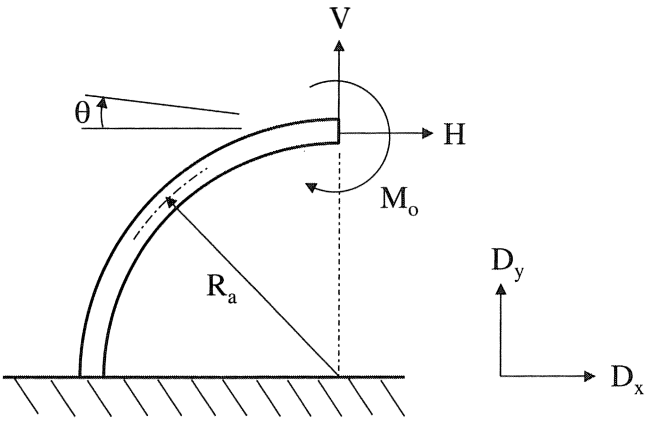

Figure A-1. Free Body Diagram of a Symmetrical Curved Beam.

REFERENCES

Gunter, E. J., Jr., Barrett, L. E., and Allaire, P. E., 1975, "Design and Application of Squeeze Film Dampers for Turbomachinery Stabilization," *Proceedings of the Fourth Turbomachinery Symposium,* Turbomachinery Laboratory, Texas A&M University, College Station, Texas, pp. 127-142.

Kuzdzal, M. J. and Hustak, J. F., 1996, "Squeeze Film Damper Bearing Experimental vs Analytical Results for Various Damper Configurations," *Proceedings of the Twenty-Fifth Turbomachinery Symposium,* Turbomachinery Laboratory, Texas A&M University, College Station, Texas, pp. 57-70.

Leader, M. E., Whalen, J. K., Hess, T. D., and Grey, G. G., 1995, "The Design and Application of a Squeeze Film Damper Bearing to a Flexible Steam Turbine Rotor," *Proceedings of the Twenty-Fourth Turbomachinery Symposium,* Turbomachinery Laboratory, Texas A&M University, College Station, Texas, pp. 49-58.

Nicholas, J. C., Edney, S. L., Kocur, J. A., and Hustak, J. F., 1997, "Subtracting Residual Unbalance for Improved Test Stand Vibration Correlation," *Proceedings of the Twenty-Sixth Turbomachinery Symposium,* Turbomachinery Laboratory, Texas A&M University, College Station, Texas, pp. 7-18.

Nicholas, J. C. and Kirk, R. G., 1982, "Four Pad Tilting Pad Bearing Design and Application for Multi-Stage Axial Compressors," ASME Journal of Lubrication Technology, *104,* (4).

Nicholas, J. C., Whalen, J. K., and Franklin, S. D., 1986, "Improving Critical Speed Calculations Using Flexible Bearing Support FRF Compliance Data," *Proceedings of the Fifteenth Turbomachinery Symposium,* Turbomachinery Laboratory, Texas A&M University, College Station, Texas, pp.69-78.

San Andres, L. A., 1992, "Analysis of Short Squeeze Film Dampers with a Central Groove," ASME Journal of Tribology, *114,* (4).

Young, W. C., 1989, Roark's Formulas for Stress and Strain, Sixth Edition, New York, New York: McGraw-Hill Book Company.

Zeidan, F. Y., San Andres, L. A., and Vance, J. M., 1996, "Design and Application of Squeeze Film Dampers in Rotating Machinery," *Proceedings of the Twenty-Fifth Turbomachinery Symposium,* Turbomachinery Laboratory, Texas A&M University, College Station, Texas, pp. 169-188.

ACKNOWLEDGEMENT

The authors would like to thank Don Rockefeller, Paul Fisk, and Rick Sauer, of Rotating Machinery Technology, Inc., for their invaluable assistance with the design, testing, and setup of the squeeze film damper assemblies, and Sean Franklin, of Dresser-Rand Energy Systems, for conducting the finite element analysis. They would also like to express their gratitude to all the assembly and test floor personnel at Dresser-Rand Energy Systems, for their considerable help and patience building and operating the turbine.